Hindawi Publishing Corporation
Journal of Nanomaterials
Volume 2016, Article ID 3840348, 12 pages
http://dx.doi.org/10.1155/2016/3840348

Research Article

Effects of Different Montmorillonite Nanoclay Loading on Cure Behavior and Properties of Diglycidyl Ether of Bisphenol A Epoxy

Alfred Tcherbi-Narteh, Mahesh Hosur, and Shaik Jeelani

Department of Materials Science & Engineering, Tuskegee University, Tuskegee, AL 36088, USA

Correspondence should be addressed to Alfred Tcherbi-Narteh; atcherbi-narteh@mytu.tuskegee.edu

Received 31 March 2016; Revised 6 June 2016; Accepted 19 June 2016

Academic Editor: Pashupati Pokharel

The primary focus of this study was to understand the effects of different amounts of montmorillonite nanoclay (MMT) loading on viscosity, cure behavior, reaction mechanism, and properties of diglycidyl ether of bisphenol A (DGEBA) epoxy composites. Influence of 1–3 wt.% MMT on rheological and subsequent cure behavior of SC-15 epoxy resin was studied using nonisothermal and isothermal rheometry and differential scanning calorimetry (DSC). Rheological properties were influenced by different amounts of MMT at lower shear rates prior to and during curing. Cure reaction mechanism was unaffected by different MMT concentration; however heat and activation energy of reactions increased with increasing MMT loading. Samples with 2 wt.% MMT showed highest reaction rate constant, indicative of catalytic behavior. X-ray diffraction (XRD) and transmission electron microscope (TEM) revealed mainly intercalated microstructure throughout the MMT infused epoxy composite samples irrespective of the percent loading.

1. Introduction

Potential uses of polymeric composites are widely growing due to several advantages they pose over metallic counterparts. Anticorrosive nature as well as impressive strength and stiffness to weight ratios are the important properties of polymer when reinforced with synthetic fibers compared to other engineering materials. Other material properties have also been enhanced using nanofillers such as carbon nanotubes, nanofibers, nanocellulose, and nanoclays [1–5]. Enhanced polymer properties include mechanical [4, 6, 7], electrical, thermal, and barrier properties [8–10], mainly through interactions between filler materials and their respective host polymers. Most targeted properties are based on inherent properties of the reinforcing fillers and their successful dispersion, exposing large surface areas of the fillers to partake in chemical reactions with the polymer molecules. Nanoclays have gained considerable attention as reinforcing fillers due to their large surface area and significant property enhancements compared to polymer composites without reinforcement [1, 2, 4]. They are naturally abundant, relatively cheaper, and easy to process with the potential to minimize effects of environmental elements on durability of polymer composites [11–14]. Nanoclays are high aspect ratio layered platelet structures stacked together and held by Van der Waals forces. In order to enhance filler-matrix interactions surfaces of nanoclays are modified with surfactants, which reduces Van der Waals forces between the clay layers [15–17]. These surfactants increase the interlayer distance and allow epoxy molecules to percolate and form different microstructures [4, 15, 18]. The extent of clay platelets delamination by epoxy molecule penetration results in exfoliated, intercalated, or flocculated microstructures, and subsequent particle-molecules interactions facilitate property enhancements [1, 2, 4]. In most polymer-filler systems, exfoliated microstructure is most desirable to fully harness properties of filler materials in polymer composites.

Nanoclays are generally characterized by their cation exchange capacity (CEC), which are based on the soil from which they are obtained. CEC dictates the amount of organic

modifiers that can be used during surface modifications and plays important role in formulating the final properties of polymer layered silicate (PLS) composites. Xidas and Triantafyllidis [16] in a study established a correlation between surface modifications and exfoliation of nanoclay in polymer matrix microstructures. Mechanism of nanoclay exfoliation in polymer was also studied by Park and Jana [8] and reported that temperature along with chain length of organic modifier influenced the resulting microstructure and rate of polymerization. Wang et al. [15] also conducted similar investigations and concluded that type of amine curing agent and rate of chemical reaction are key factors in the formation of exfoliated microstructure. Surface modifications and processing techniques have also been identified as key factors affecting mobility of nanoclay particles during dispersion, influencing viscosity and cure behavior, including rate of conversion (catalytic), cross-linking, and overall properties of the final composites [16, 18–23].

Optimization of properties of MMT infused polymer composites may require different processing parameters based on overall concentration of MMT present. This requires an in-depth understanding of the effects of different concentration of MMT during curing and development of material properties. Hence in the current study, effects of 1–3 wt.% MMT loading on the cure behavior, reaction mechanism, and development of composite material properties of epoxy resin were studied using isothermal and nonisothermal differential scanning calorimetry (DSC) and rheometry. Furthermore, their influence on viscoelastic properties of epoxy composites was studied using dynamic mechanical analysis (DMA).

2. Experimental

2.1. Materials and Fabrication of Nanocomposites

2.1.1. Materials. Two parts, diglycidyl ether of bisphenol A (DGEBA) epoxy resin SC-15 (part A) and proprietary cycloaliphatic amine curing agent (part B), were supplied by Applied Poleramic Inc. Montmorillonite nanoclay (MMT) with 25–30 wt.% trimethyl stearyl ammonium surface modification and cation exchange capacity (CEC) of 93.7 mequiv/100 g was acquired from Sigma Aldrich.

2.1.2. Sample Fabrication. Samples for the study were fabricated using varying concentration of MMT dispersed into measured amounts of epoxy SC-15 resin part A using magnetic stirring technique at 500 rpm for 24 hours to form mixtures of 1, 2, and 3 wt.% MMT reinforced epoxy resin. Samples denoted by 0 wt.% MMT represent epoxy samples without MMT, while 1, 2, and 3 wt.% MMT represent SC-15 epoxy samples infused with 1, 2, and 3 wt.% MMT, respectively. Stoichiometric amount of part B (curing agent) was then added to each MMT/epoxy mixture, mechanically stirred for about 3 minutes and degassed for a few minutes. Rheology and thermal analyses were performed using small amount of uncured MMT/epoxy mixture to determine the cure kinetic parameters. Part of the resin was poured into molds and cured at room temperature for 24 hours followed by 2 hours after curing in a conventional oven set at 80°C to form unmodified and MMT reinforced epoxy composites. The above cure schedule is according to prescribed manufacturer's curing cycle.

2.2. Characterization Techniques

2.2.1. X-Ray Diffraction (XRD). XRD analyses of cured MMT infused epoxy composite samples were done using Rigaku-DMAX-2000 with Cu Kα radiation of wavelength λ = 1.54 nm, operating at 40 kV and 30 A. Separate XRD studies were performed on thin layer of MMT powder uniformly spread across XRD sample holder, and square MMT infused cured composite samples machined from each sample set. Each sample was polished to reduce sample thickness to 2-3 mm and placed in sample holder for scanning. Three samples from each composite considered under the study were scanned from 2 to 40° at a scan rate of 0.2° and diffraction peaks analyzed for comparison.

2.2.2. Transmission Electron Microscopy (TEM). Further microstructural analyses were done on MMT infused samples using Zeiss EM 10 TEM equipment with accelerating voltage set at 100 kV. Several TEM samples were cut from each composite at 25°C using ultramicrotome equipped with diamond cutter, with sample thickness ranging between 50 and 100 nm. Micrographs were obtained from several samples of each MMT infused sample set for analyses and comparison.

2.2.3. Rheology. Rheological studies on SC-15 epoxy resin including those infused with MMT were conducted using TA Instruments AR 2000 equipped with environmental test chamber (ETC). Disposable 25 mm aluminum plates with a drip on the bottom plates were used throughout the tests. Three freshly mixed part A and B epoxy resin samples including MMT modified epoxy resin were used during each test. Shear rate dependency experiment was carried out at 25°C from 0.01 to 100 rads^{-1} with oscillating maximum normal force of 5.0 N. Dynamic cure temperature ramp investigations were performed on each uncured epoxy resin sample from 30 to 180°C at 5°C/min, while isothermal curing was investigated at 60, 70, 80, and 90°C in oscillation-time-sweep mode. A small sinusoidal shear strain of 1% was applied to the parallel plates at a constant shear rate of 6.23 rads^{-1} during each test.

2.2.4. Differential Scanning Calorimetry (DSC). Differential scanning calorimetry (DSC) studies were performed using TA Instruments' DSC Q2000. Cell constant and temperature sensitivity of the instrument were calibrated using sapphire and indium metal samples, respectively, and purged with dry nitrogen at 50 mL/min. A set of three samples was tested from each sample set, and data from each scan were analyzed using TA Instruments' Universal Analysis software.

2.2.5. Dynamic Mechanical Analysis (DMA). Effects of varying amount of MMT infusion on viscoelastic properties of SC-15 epoxy resin composites were investigated using

dynamic mechanical analysis (DMA) equipment Q800 from TA Instruments'. The DMA equipment was operated in a dual cantilever mode at a frequency of 1 Hz and amplitude of 15 μm. Three sets of samples were tested from each sample set at a ramping rate of 5°C/min from 30 to 180°C. Storage modulus at 30°C was recorded for each experiment and average data presented for comparison along with average data from glass transition temperatures for each sample set. Glass transition temperature was determined from peak of tan delta curve according to ASTM D4065-06 [24].

3. Cure Reaction

Influence of different amounts of MMT loading on SC-15 epoxy cure reactions was investigated using DSC scans, and data from the scans was analyzed using isoconversional models. In DSC scans, rate of chemical conversion ($d\alpha/dt$) of epoxy during curing is proportional to the measured heat flow rate (dH/dt) relative to the baseline of the instrument and expressed as

$$\frac{d\alpha}{dt} = \frac{dH/dt}{\Delta H}, \tag{1}$$

where ΔH is total heat generated from the reaction to reach full conversion.

Furthermore, kinetic analysis of chemical reaction during curing in DSC can be described as a function of conversion fraction (α) and temperature (T), which is often expressed as

$$\frac{d\alpha}{dt} = k(T)\, f(\alpha), \tag{2}$$

where $f(\alpha)$ is a function representing reaction model and $k(T)$ is a temperature-dependent function expressed in Arrhenius form:

$$k(T) = A \exp\left(-\frac{E_a}{RT}\right). \tag{3}$$

Therefore (2) can be expressed as

$$\frac{d\alpha}{dt} = A \exp\left(-\frac{E_a}{RT}\right) f(\alpha), \tag{4}$$

where A is preexponential factor, E_a is apparent activation energy, R is universal gas constant (8.3144 KJ/mol), and T is absolute temperature (K). Introducing the heating rate ($\beta = dT/dt$) and rearranging (4) yield the following equation:

$$\beta \frac{d\alpha}{dT} = A \exp\left(-\frac{E_a}{RT}\right) f(\alpha). \tag{5}$$

For dependency of MMT loading on activation energy (E_a) of reaction, isoconversional integral method Kissinger-Akahira-Sunose (KAS) was used to analyze nonisothermal scanning data, which require several experiments at different temperature scans as emphasized by Vyazovkin et al., 2011 [25]. Using this integral method activation energy of reaction was determined from the slope of linear fit from plots of $\ln(\beta/T_p^{1.92})$ versus $(1/T_p)$ at different heating rates as shown by Starink (2003) [26] and expressed in (6). Furthermore, using (4) activation energy (E_a) can be determined as function of degree of conversion (α) using Friedman differential method expressed in (7). Consider

$$\ln\left(\frac{\beta}{T_P^{1.92}}\right) = \text{const} - 1.0008\frac{E_a}{RT_P}, \tag{6}$$

$$\ln\left(\frac{d\alpha}{dt_\alpha}\right) = \ln\left[Af(\alpha)\right] - \frac{E_\alpha}{RT_\alpha}. \tag{7}$$

During isothermal curing, dependency of cure rate ($d\alpha/dt$) and degree of cure (α) can be expressed according to Kamal's model using (2) and (3) as follows:

$$\frac{d\alpha}{dt} = \left(k_1 + k_2\alpha^m\right)(1-\alpha)^n, \quad \text{where } k_1 = A_1 e^{(-E_{a1}/RT)},\ k_2 = A_2 e^{(-E_{a2}/RT)}, \tag{8}$$

where m and n are the reaction orders and k_1 and k_2 are reaction rate constants. k_1 represents the kinetic rate constant related with the noncatalytic reaction between the epoxide and amine groups related to partial order "n" based on the initial rate $\alpha = 0$. k_2 is the rate constant due to the hydroxyl group formed as a result of catalytic effect of amine curing agent and related to partial order m.

4. Results and Discussion

4.1. Microstructural Analysis. Property enhancement in PLS composites has been attributed to several factors including the surface modification, degree of dispersion of the MMT, and most importantly chemical compatibility between MMT particles and polymer molecules [16, 20, 27]. These factors drive clay-epoxy interaction leading to increase in interlayer spacing caused by movement of epoxy molecules. As a result different microstructures with distinct characteristics and properties are obtained and reported in literature [5, 20, 28]. XRD results show distinct basal characteristic reflections of MMT shown in Figure 1(a), while single broad peaks with varying intensities were obtained from each MMT infused composite sample, indicative of intercalated microstructure. Interlayer d-values determined from each basal reflection using Bragg's law were 7.9, 21.0, 16.3, and 16.1 Å for MMT powder, 1, 2, and 3 wt.% MMT loaded epoxy composites, respectively. The absence of MMT characteristic peaks in MMT infused epoxy resin composites is indicative of good dispersion (Figure 1(a)). However displacement of diffraction peak and presence of broader peak with varying d-values are indicative of successful intercalation. To further substantiate this, TEM micrographs (Figures 1(b)–1(d)) were obtained randomly, throughout each MMT composite sample for qualitative analysis of spatial distribution of MMT. The micrographs showed mainly intercalated microstructures for 2 and 3 wt.% samples and relatively higher dispersion in 1 wt.% sample (Figure 1(b)).

4.2. Rheological Characterization

4.2.1. Shear Rate Dependency. Changes in viscosity of epoxies due to nanoclay infusion including self-polymerization and

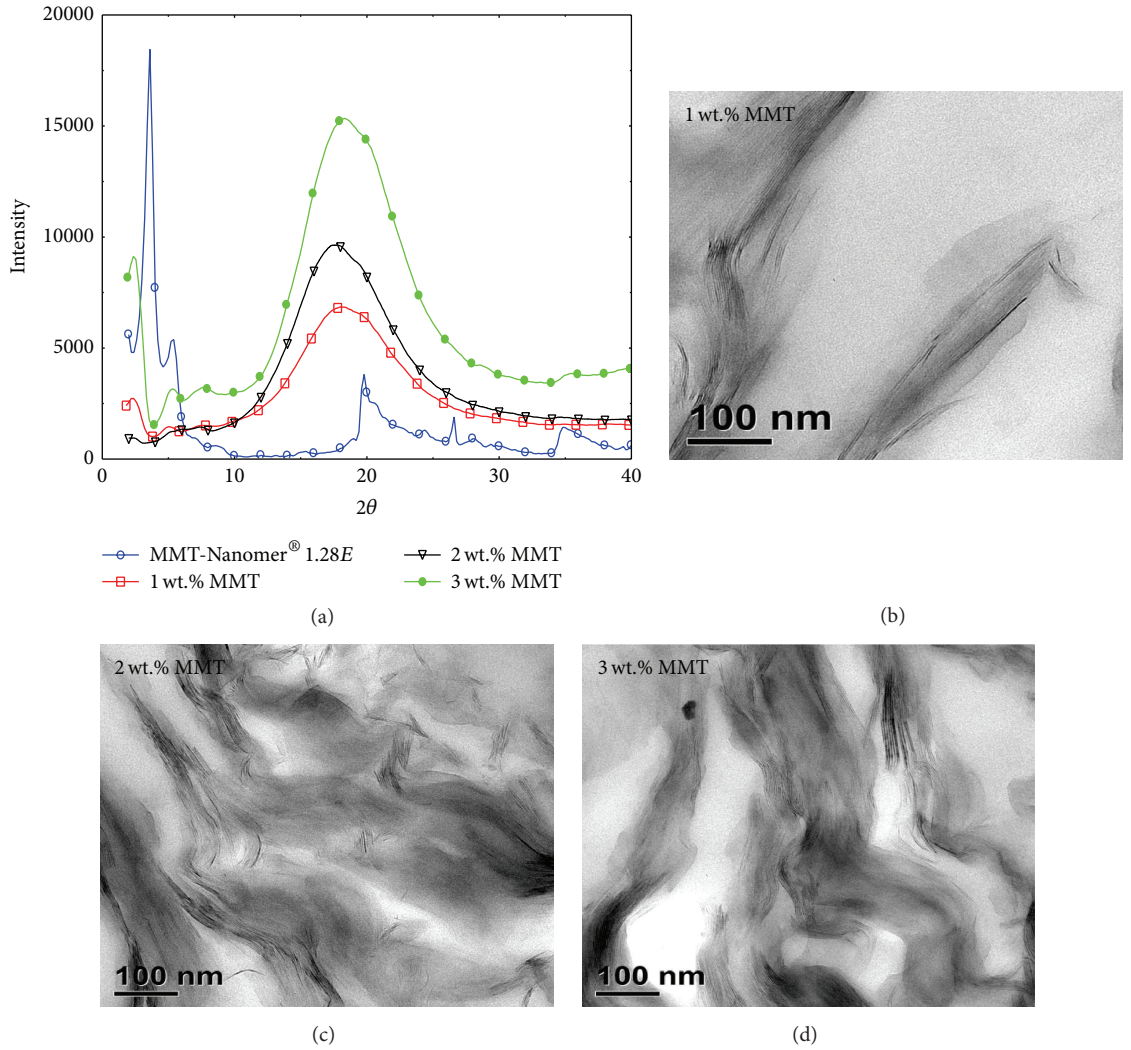

FIGURE 1: Microstructural analysis: (a) XRD patterns of MMT powder, 1, 2, and 3 wt.% MMT infused composites; and (b–d) TEM of 1, 2, and 3 wt.% MMT infused composites, respectively.

their influence on curing have been well documented [5, 27–29]. Dependency of viscosity on shear rate was studied at room temperature on mixtures of part A SC-15 modified with MMT samples without part B and shown in Figure 2 with average data in Table 1. Interactions between extremely small MMT particles and epoxy molecule at shear rates between 0.1 and 5 s^{-1} were dominated by chemical interactions, while that beyond 5 s^{-1} was mainly hydrodynamic or shear force due to lack of interaction between clay particles and epoxy molecules [9, 30, 31]. The small amount of particles in each system and their interactions with one another resulted in the opening of interlayer spacing of the MMT particles and subsequent movement of epoxy molecules into the layers. As a result morphology and non-Newtonian behavior of MMT infused systems particularly between 2 and 3 wt.% samples are observed [28, 32, 33]. Nanoclay particles under the influence of shear force can reorient and align themselves providing a plane for smooth response to external shear stress exerted by the parallel plates resulting in lower viscosity particularly at higher shear rate between 20 and 100 s^{-1} [33, 34]. The similarity in viscosity responses to shear stress among all samples beyond 20 s^{-1} can be ascribed to characteristic behavior of SC-15 epoxy resin with 3 wt.% samples showing highest values due to anisotropic microstructure [31]. Furthermore, these interactions revealed characteristic responses of SC-15 epoxy resin to shear stress at specific shear rates independent of MMT loading.

4.2.2. Nonisothermal Temperature Studies. Viscosity and subsequent developments of MMT infused SC-15 composite properties during curing were monitored using nonisothermal curing rate at 5°C/min. Figure 3 shows representative curves of viscosity as function of temperature for different MMT loadings and average cure characteristic parameters are presented in Table 2. Changes in viscosity due to interactions between clay particles and epoxy molecules at increasing temperatures affected the process of gelation, vitrification, and formation of final properties compared to unmodified

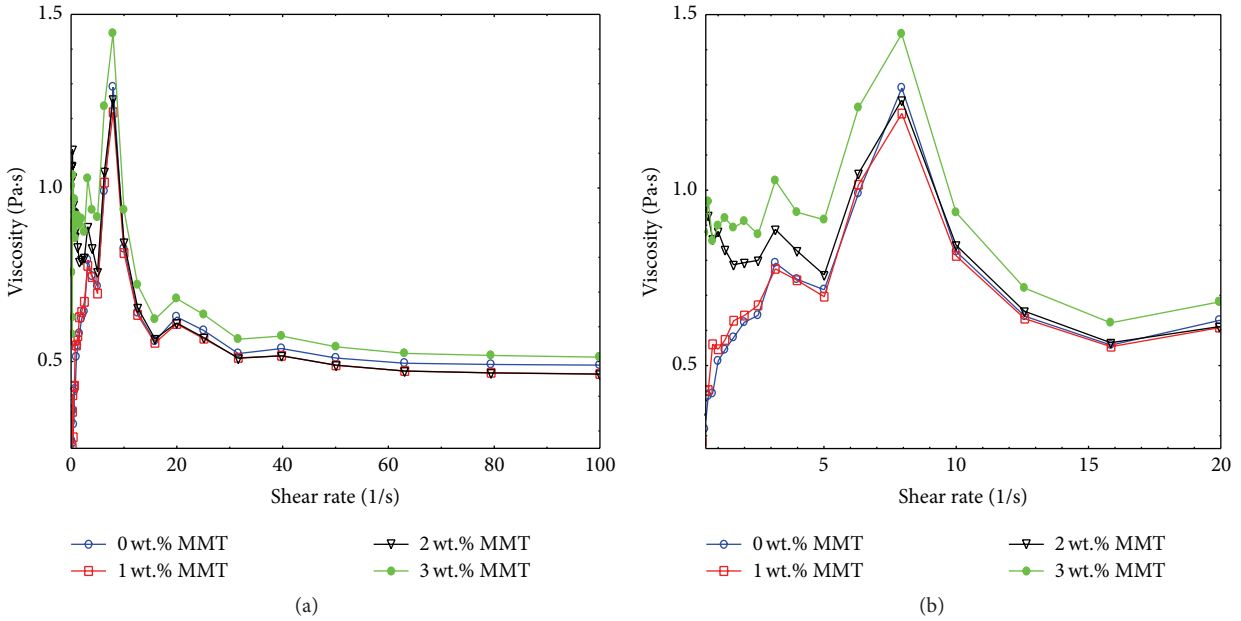

Figure 2: Viscosity measurements at varying shear rate for unmodified and MMT modified composites between (a) 0 and 100 s^{-1} and (b) 0 and 20 s^{-1}.

Table 1: Summary of rheological studies at room temperature.

Sample/shear rate, 1/s	Viscosity at various shear rates, μPa·s			
	Unmodified SC-15	1 wt.% MMT	2 wt.% MMT	3 wt.% MMT
1	512.5 ± 14.1	553.3 ± 42.3	855.7 ± 32.7	814.2 ± 12.5
5	723.3 ± 29.7	708.3 ± 52.8	764.4 ± 11.2	856.2 ± 153.3
8	1291.0 ± 37.6	1221.0 ± 83.7	1248.7 ± 21.9	1441.3 ± 130.3
10	820.8 ± 35.2	813.8 ± 47.2	839.7 ± 11.7	63.4 ± 158.9
20	628.7 ± 23.3	609.6 ± 35.0	614.7 ± 12.4	648.0 ± 99.8
100	489.5 ± 16.0	466.2 ± 28.1	467.5 ± 11.9	483.7 ± 82.6

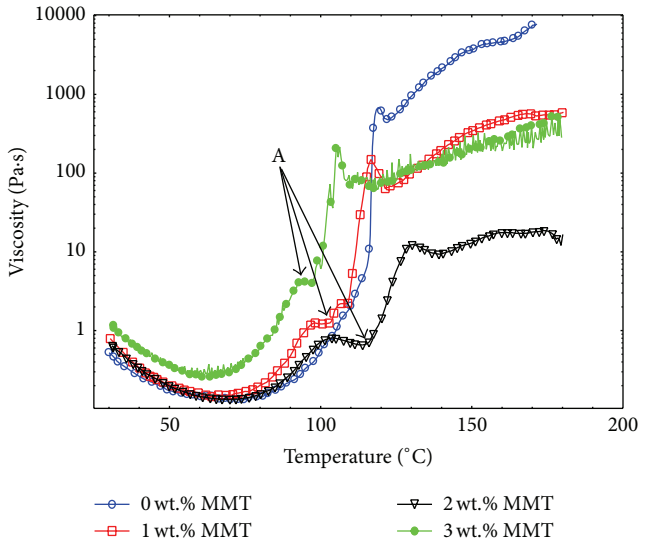

Figure 3: Viscosity dependency on dynamic curing temperature at 5°C/min.

system [19, 27]. At the onset of each experiment nanoclay swelling, tethering, and formation of clay particle network in the modified systems lead to an increase in viscosity compared to unmodified system. The swelling can further expose more unreactive nanoclay surfaces, thus increasing chemical interactions with epoxy molecules and resulting in enhanced catalytic behavior of MMT. This behavior has been attributed to quantity of alkyl ammonium ions used in clay surface modification, MMT concentration, and cure temperature [15, 19, 20]. Varying MMT content disrupted the process of gelation indicated by "A" (Figure 3) in each modified system during curing. Gel temperature was measured as temperature where viscosity became independent during curing and average data reported in Table 2 [33].

The results showed that gelation occurred at relatively lower temperatures for 1 and 3 wt.% and higher for 2 wt.% samples compared to unmodified system. It was assumed that delay in gelation of 2 wt.% samples was caused by epoxy molecules trapped between layers. At this point, although temperature was increasing during curing, changes in viscosity were unnoticeable since this was occurring at the

Table 2: Summary of dynamic rheological curing.

Sample	Viscosity at 30°C, μPa·s	Lowest viscosity, μPa·s	Temperature at lowest viscosity, °C	Gel temperature, °C
0 wt.% MMT	440.3 ± 6.1	72.9 ± 15.0	68.7 ± 1.4	111.8 ± 4.2
1 wt.% MMT	621.1 ± 18.4	115.5 ± 34.0	75.8 ± 2.9	112.0 ± 3.4
2 wt.% MMT	685.1 ± 19.6	137.7 ± 19.8	69.3 ± 1.3	124.1 ± 1.3
3 wt.% MMT	864.7 ± 26.9	283.4 ± 14.4	59.2 ± 1.7	105.7 ± 2.2

microstructural level [35]. This interruption in gelation further influenced vitrification and development of material properties as can be expected. Epoxy molecular transition from gelation to vitrification is an event influenced by molecular weight and restrictive molecular movements enhanced by concentration of MMT and growing network of chain segments [19, 20, 27, 36]. Furthermore, this can lead to catalytic behavior of MMT which was observed particularly in 2 wt.% samples compared to other nanoclay loaded samples. Vitrification occurred at lower viscosities for 2 wt.% samples followed by 3 and 1 wt.% samples caused by delayed epoxide conversion due to entrapped molecules between the intergallery spacing [16]. Minimum viscosities for each system attained at different times and temperatures during scanning are indications of varying effects of different MMT content on curing and evolution of the physical properties.

4.2.3. Isothermal Temperature Studies. Summary of isothermal rheological studies presented in Table 3 further demonstrates influence of varying MMT content on viscosity and gel point as function of isothermal temperature. Gel point, determined from the crossover point between storage and loss moduli curves where epoxy undergoes structural changes, showed a decreasing trend with increasing cure temperature. This was expected due to enhanced chemical interaction leading to increased reactivity and formation of chain networks or cross-linking with increasing temperature [32, 34]. Viscosity of each system at gel point varied significantly based on MMT composition, conversion, and temperature, with no particular trend observed (Table 3), thus validating the complexities involved in epoxy curing [20, 37].

Gelation and degree of cure at gel point (α_{gel}) depend on chemical structure and functionalities of the epoxy system and according to Flory's theory of gelation [38], the process is constant regardless of the isothermal cure temperature and can be expressed as

$$t_{\text{gel}} = \frac{1}{K(T)} \cdot \int_0^{\alpha_{\text{gel}}} \frac{1}{g(\alpha)} d\alpha, \tag{9}$$

$$\ln\left(t_{\text{gel}}\right) = \ln\left[\frac{1}{A_o}\left(\int_0^{\alpha_{\text{gel}}} \frac{1}{g(\alpha)} d\alpha\right)\right] + \frac{E_a}{R} \cdot \frac{1}{T}, \tag{10}$$

where A_o is preexponential factor at $t = 0$ and α_{gel} is the conversion at gel point.

Hence apparent activation energy of reaction can be determined from the slope of linear fit from experimental plots of $\ln(t_{\text{gel}})$ versus reciprocal of absolute curing temperature $(1/T)$ using (10) and the results reported in Table 3. Physical properties of epoxy composites during curing are influenced by viscosity and vitrification; hence changes in viscosity caused by varying MMT content can disrupt the molecular transformation from rubbery to glassy states and its optimization. From the study it was observed that at relatively lower temperature (60 and 70°C), influence of MMT on viscosity and gelation was more pronounced and became less influential at elevated temperatures 80 and 90°C due to increased kinetic energy of the reaction species. Hence varying MMT content may affect reaction rate and formation of cross-linking as well as properties of the final composites at these temperatures.

4.3. DSC Measurement

4.3.1. Dynamic Scans. A single exothermic peak was obtained for all SC-15/MMT systems during scanning with varying intensity based on the heating rate. Plots of conversion (α) as function of temperature for each system during curing shown in Figure 4(a) with identical characteristics are indicative of autocatalytic cure behavior [20, 25]. This similarity in cure profiles underscores the lack of MMT influence on overall cure reaction mechanism of SC-15 epoxy system as previously asserted, regardless of the MMT content. However, the presence of different MMT concentration affected other cure parameters such as reaction rate, heat, and activation energy of reactions. Heat of reaction and activation energy increased with increasing clay content due interactions between the nanoclay particles and epoxy molecules in all MMT infused epoxy composites compared to unmodified systems. Activation energy of reaction for all systems determined using KAS method was approximately 50, 51, 60, and 61 kJ/mol for 0, 1, 2, and 3 wt.% MMT reinforced epoxy systems, respectively (Figure 5). Further investigation of activation energy dependency on conversion (α) was done using isoconversional differential (Friedman) method shown in Figure 6 where activation energy (E_α) obtained from linear fit of data ($0.1 \leq \alpha \leq 0.95$) was plotted as function of conversion (α) in Figure 7.

For comparison, activation energy was determined at 5% conversion for all samples and reported as 40, 43, 56, and 51 kJ/mol for 0, 1, 2, and 3 wt.% MMT reinforced epoxy systems, respectively. These results followed similar trend from those obtained using the integral method earlier. Activation energy gradually increased for unmodified and 1 wt.% MMT modified systems till approximately 60% conversion. Samples with 3 wt.% MMT initially decreased up to 20% conversion and remained unchanged till about 60% and significantly increased beyond 80% conversion. Activation energy of samples with 2 wt.% MMT reinforcements remained statistically unchanged from the onset of conversion till 60% conversion and gradually reduced showing a

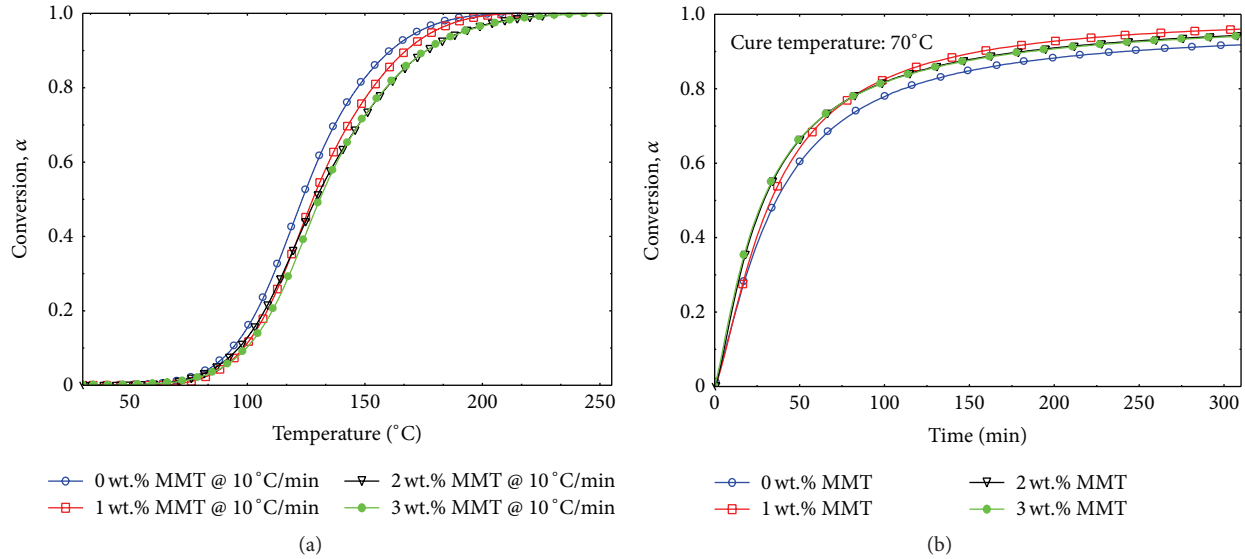

FIGURE 4: Influence of MMT on reaction mechanism: plots of conversion (α) as function of (a) temperature during scanning at 10°C/min and (b) time during isothermal curing at 70°C.

TABLE 3: Summary of isothermal rheological curing studies.

Sample	Cure temperature, °C	Gel time, s	Storage modulus at gel point, Pa	Viscosity at gel point, Pa·s	Activation energy E_a, KJ/mol
0 wt.% MMT	60	3456 ± 160	43810 ± 120	9844 ± 246	69.59 ± 1.78
	70	1801 ± 94	30380 ± 167	6882 ± 161	
	80	1001 ± 69	8884 ± 149	2977 ± 201	
	90	391 ± 38	4606 ± 192	1027 ± 88	
1 wt.% MMT	60	5821 ± 141	84650 ± 305	19010 ± 109	65.26 ± 2.40
	70	2981 ± 39	24440 ± 293	5492 ± 207	
	80	1631 ± 48	8106 ± 150	1808 ± 86	
	90	801 ± 21	4665 ± 101	1031 ± 44	
2 wt.% MMT	60	5851 ± 127	98170 ± 119	22570 ± 366	65.93 ± 1.9
	70	3131 ± 44	28260 ± 246	6109 ± 127	
	80	1491 ± 29	12010 ± 83	2138 ± 87	
	90	841 ± 33	4767 ± 77	1073 ± 44	
3 wt.% MMT	60	5491 ± 97	113300 ± 228	25510 ± 180	68.17 ± 1.97
	70	2591 ± 131	36685 ± 311	7920 ± 179	
	80	1471 ± 49	12700 ± 108	2867 ± 112	
	90	691 ± 37	5588 ± 98	1296 ± 66	

reverse trend compared to the others. The observed behavior among MMT infused samples underscores the complexities involved in epoxy thermosets curing with or without fillers, and 2 wt.% samples showed catalytic characteristics at higher conversion [19]. Cure mechanism of epoxy molecules at this stage was controlled by diffusion, and lower activation energies exhibited by 2 wt.% samples are indicative of hindering effects of MMT on vitrification. Trapped epoxy molecules and tethering network within nanoclay layers in 2 wt.% samples produced sufficient hydroxyl groups during vitrification [35]. This facilitated the process and thus less energy was necessitated during diffusion controlled reaction as seen in Figure 7. This observation corroborate results from rheological studies (Figure 3) where vitrification occurred at much lower viscosity compared to the other systems. Amount of MMT presence in 1 wt.% also suggests longer molecular chain length caused by formation of tethering network due to exfoliation and resulting in lower resistance to mobility compared to 2 and 3 wt.% systems. As a result relatively higher energy was required to fuse MMT/epoxy molecules together during vitrification to increase the cross-linking density. This observation once again reaffirms the prospects of using different cure parameters for nanoclay infused epoxy thermosets for optimization of material properties.

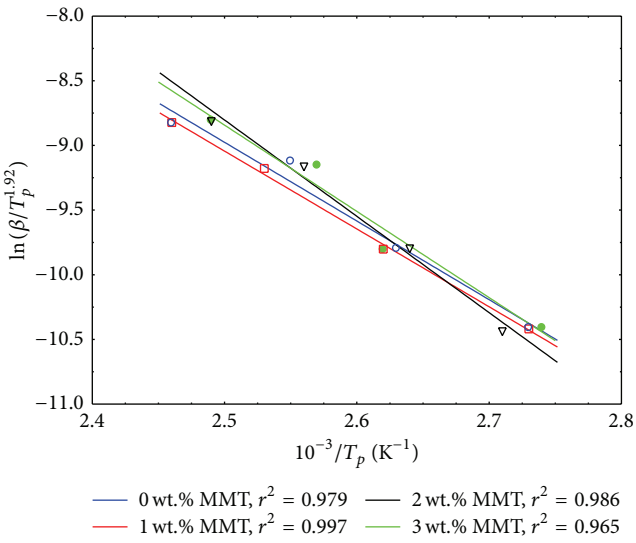

FIGURE 5: Determination of activation energy from Kissinger-Akahira-Sunose model.

Heat of reactions was approximately 309, 328, 360, and 381 J/g for 0, 1, 2, and 3 wt.% MMT infused compositions, respectively, showing an increasing trend with increasing MMT content. It can be hypothesized that clay/epoxy interaction may have changed the concentration of reactive groups and led to changes in stoichiometric ratio of epoxy resin (part A) and curing agent (part B). Although this cannot be confirmed, it can be assumed that epoxy molecules trapped in the interlayer spaces of the MMT particles and their subsequent interactions may have led to reduction of epoxy SC-15 part A molecules available to react with stoichiometric part B. Furthermore, morphology of MMT may have prevented heat from reaching entrapped molecules at the onset of curing, and more heat was released as the entrapped molecules began to cure at the later stage of the curing. Hence the system may require different stoichiometric amount of part B, based on MMT content, and may require different processing time necessary to bring the reacting species together.

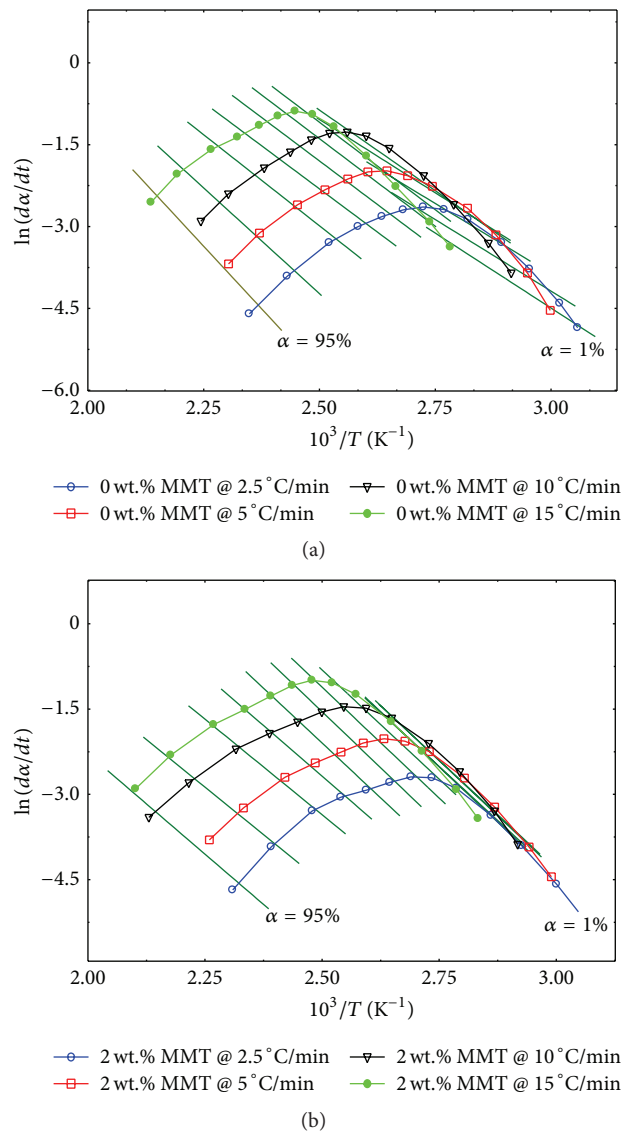

FIGURE 6: Representative plots of $\ln(d\alpha/dt)$ versus $1/T$ curves for (a) 0 wt.% MMT (unmodified) and (b) 2 wt.% MMT modified epoxy samples.

4.3.2. Isothermal DSC Scan. Results from isothermal studies revealed identical thermograms with similar characteristic features of the reaction curves during curing (Figure 4(b)). This indicates the lack of influence on the reaction mechanism by various amounts of MMT loading. However cure parameters such as time for each composition to reach the maximum peak occurred at different times based on the constituents and decreased with increasing clay content. Average data from heat of reaction shown in Table 4 also followed similar trend reported earlier during dynamic DSC and rheological studies. TA Instruments' Specialty Library software was used to generate conversion time-temperature curves for all systems and Figures 8(a) and 8(b) show representative curves for unmodified and 2 wt.% MMT modified epoxy composite samples. Evidence of MMT's influence on cure behavior of SC-15 epoxy resin system on reaction can be seen from Figure 8, where time and temperature to reach specific conversion varied from system to system. The results also showed that 2 wt.% MMT infused samples displayed most catalytic effect throughout the cure process. This was evident in increased reaction rate constant (k) and minimum values of reaction order (m) parameter (Table 4) compared to other samples including unmodified epoxy composites regardless of the curing temperature. Also, time to reach maximum conversion (T_p) was observed to be lower in 2 wt.% systems compared to unmodified and other nanocomposite systems except 3 wt.% at 90°C.

Epoxy cure reactions involving amines curing agents have been generally considered to be autocatalytic as observed throughout the study, with overall reaction orders ($m + n$) assumed to be 2 [20, 27, 39]. Hence appropriate cure temperature and corresponding time to cure each sample with autocatalytic behavior were determined using results from

Table 4: Summary of isothermal cure studies.

Samples	Parameter	Isothermal temperature, ˚C			
		60	70	80	90
0 wt.% MMT	n	1.15 ± 0.053	1.66 ± 0.096	1.72 ± 0.065	2.44 ± 0.12
	m	0.311 ± 0.029	0.26 ± 0.052	0.298 ± 0.035	0.308 ± 0.068
	K ($\times 10^{-3}$)	24.0 ± 2.0	33.0 ± 4.0	73.0 ± 6.0	94.0 ± 14.0
	T_p, min	32.53	19.93	13.37	12.70
	ΔH, J/g	301.10	444.04	351.36	429.27
1 wt.% MMT	n	1.43 ± 0.044	1.76 ± 0.063	1.96 ± 0.11	1.55 ± 0.05
	m	0.316 ± 0.024	0.252 ± 0.034	0.222 ± 0.062	0.284 ± 0.029
	K ($\times 10^{-3}$)	23.0 ± 1.0	39.0 ± 3.0	59.0 ± 8.0	141.0 ± 9.0
	T_p, min	30.55	15.17	12.42	11.20
	ΔH, J/g	374.55	408.9	432.21	329.18
2 wt.% MMT	n	1.61 ± 0.05	1.70 ± 0.12	2.09 ± 0.10	2.70 ± 0.08
	m	0.232 ± 0.03	0.036 ± 0.067	0.158 ± 0.056	0.281 ± 0.045
	K ($\times 10^{-3}$)	33.0 ± 2.0	61.0 ± 4.0	82.0 ± 7.0	127.0 ± 12.0
	T_p, min	15.85	10.60	9.70	9.82
	ΔH, J/g	442.54	460.68	473.95	511.97
3 wt.% MMT	n	1.53 ± 0.054	1.94 ± 0.68	2.03 ± 0.072	2.25 ± 0.073
	m	0.250 ± 0.023	0.275 ± 0.037	0.232 ± 0.039	0.187 ± 0.040
	K ($\times 10^{-3}$)	27.0 ± 2.0	52.0 ± 4.0	72.0 ± 6.0	105.0 ± 9.0
	T_p, min	20.55	13.20	10.03	8.92
	ΔH, J/g	446.17	386.72	478.19	407.58

Table 5: Summary of viscoelastic properties as function of MMT loading.

Sample	Storage modulus, MPa	% change	Glass transition temperature, ˚C	% change
0 wt.% MMT	1995.0 ± 56.0	—	98.8 ± 0.4	—
1 wt.% MMT	2239.5 ± 0.5	12.3	110.8 ± 0.6	11.8
2 wt.% MMT	2035.5 ± 24.5	2.0	111.6 ± 1.1	12.9
3 wt.% MMT	2133.7 ± 102.2	6.9	114.2 ± 2.6	15.6

Table 4 and the curves from Figure 8. Furthermore, temperatures at which reaction orders of each system were closest to 2 were determined for autocatalytic behavior; thus $m + n = 2$. Proposed reaction temperature for unmodified system was 80˚C, 1 and 2 wt.% MMT systems 70˚C, and 3 wt.% MMT system 60˚C. It follows that proposed temperature for curing decreased with increasing MMT content. This validates the effects of chemical interactions between the MMT particles and epoxy molecules seen earlier during curing. Furthermore, using the curves in Figure 8, corresponding cure time for various percent conversions can be established. For example, in order to cure each of the systems under the study to 95% conversion based on the proposed reaction orders and temperatures mentioned above, the stipulated time will be 3.54, 4.45, 7.62, and 8.64 hours for 0, 1, 2, and 3 wt.% MMT infused epoxy resin, respectively. Hence for optimization of material properties of nanoclay infused epoxy polymeric composites, different cure parameters may be required other than manufacturers' recommended cycle. Furthermore, a dependency of reaction orders (m and n) on curing temperatures can be established especially the parameter n as presented in Table 4. While no particular trend was observed in the values of m, it however confirms the complexities involved in epoxy curing [20, 39].

4.4. Influence of MMT on Viscoelastic Properties. Effects of different amounts of MMT on viscoelastic properties of PLS were studied using dynamic mechanical analysis (DMA) on all samples cured using manufacturer's recommended cycle. DMA scans performed from 30 to 180˚C showed influence of MMT on storage modulus and damping effects compared to that of unmodified SC-15 epoxy composite samples presented in Table 5. Results from DMA test points to MMT particles facilitating the interlocking of the polymer molecular chain, leading to increased strength and restrictive mobility of the molecules at elevated temperature. This led to observed increase in glass transition temperature with increasing MMT content. It also showed that these bonds could be enhanced if proper parameters had been used during curing as suggested based on studies from previous sections. Storage modulus on the other hand showed a 12% enhancement in 1 wt.% MMT infused samples, which was attributed to higher degree of exfoliation due to relatively small amount of MMT in the

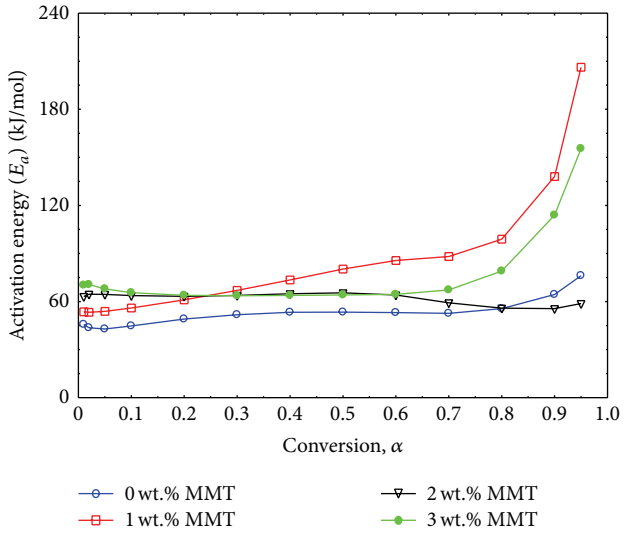

FIGURE 7: Plots of activation energy as function of conversion (α) for 0 (unmodified), 1, 2, and 3 wt.% MMT infused epoxy samples.

mixture. The results further validate the assertion that properties of PLS composites are dictated by degree of interaction between the nanoparticles used as fillers and host polymer, affecting the rate of chemical reaction and properties of final products [19, 23, 35]. Average glass transition determined from rerun of DSC scans of isothermally cured samples at 5°C/min also showed an increasing trend with increasing MMT content, thus 5.58, 6.63, and 7.33% for 1, 2, and 3 wt.% MMT, respectively. To validate the results from isothermal DSC, samples were fabricated and cured to 95% conversion using parameters based on $(m + n) = 2$ discussed in the previous section. Glass transition temperature obtained from DSC scans showed enhancement of 7, 13, and 11% and approximately 11, 19, and 14% from DMA test for 1, 2, and 3 wt.% MMT, respectively, compared to systems cured according to manufacturers' cycle.

5. Conclusion

Influence of MMT on the cure behavior of DGEBA epoxy resin SC-15 was investigated using dynamic and isothermal rheometry and DSC, respectively. Viscosity of SC-15 epoxy resin was significantly affected at lower shear rates due to dominance of chemical interaction and concentration of MMT. Minimum viscosity during curing was attained at different temperatures based on percent MMT loading which affected gelation and vitrification. Overall cure reaction mechanism of SC-15 epoxy resin was unaffected regardless of percent loading of MMT; however activation energy and enthalpy of reactions increased with increasing clay content. Analyses of data from the study and cure reaction parameters indicate that properties of MMT infused polymer materials can be optimized by using different cure parameters based on concentration of MMT used as reinforcement.

Competing Interests

The authors declare that they have no competing interests.

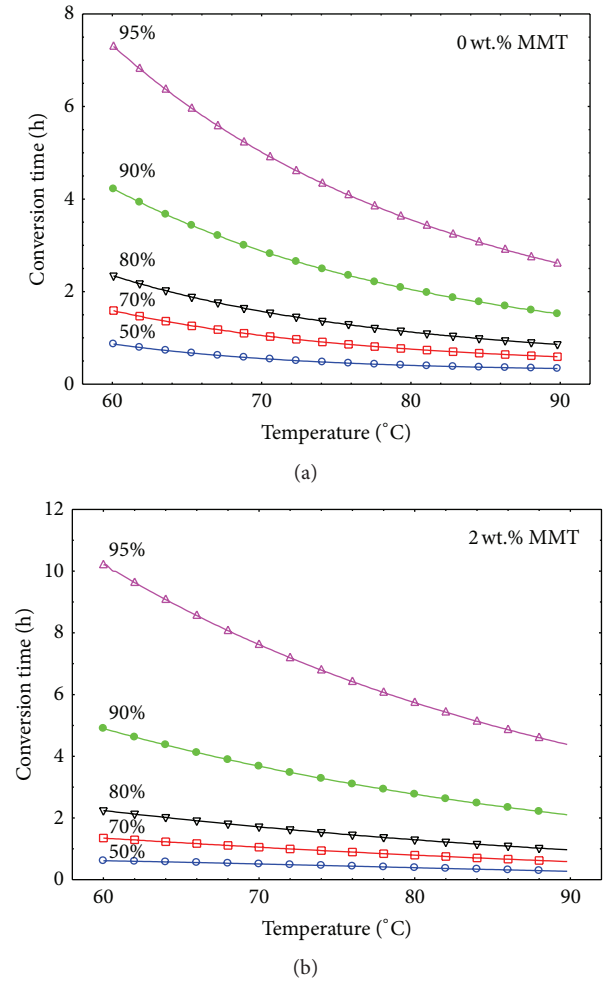

FIGURE 8: Representative plots of conversion time versus temperature for (a) 0 wt.% MMT (unmodified) and (b) 2 wt.% MMT infused epoxy system.

Acknowledgments

The authors would like to acknowledge the support from Office of Naval Research (Grant no. N00014-08-1-0665) and National Science Foundation (EPS-1158862). The first author would also like to thank Alabama Commission on Higher Education for providing graduate fellowship.

References

[1] S. Pavlidou and C. D. Papaspyrides, "A review on polymer-layered silicate nanocomposites," *Progress in Polymer Science*, vol. 33, no. 12, pp. 1119–1198, 2008.

[2] F. Hussain, M. Hojjati, M. Okamoto, and R. E. Gorga, "Review article: polymer-matrix nanocomposites, processing, manufacturing, and application: an overview," *Journal of Composite Materials*, vol. 40, no. 17, pp. 1511–1575, 2006.

[3] X. Kornmann, M. Rees, Y. Thomann, A. Necola, M. Barbezat, and R. Thomann, "Epoxy-layered silicate nanocomposites as matrix in glass fibre-reinforced composites," *Composites Science and Technology*, vol. 65, no. 14, pp. 2259–2268, 2005.

[4] M. Alexandre and P. Dubois, "Polymer-layered silicate nanocomposites: preparation, properties and uses of a new class of materials," *Materials Science and Engineering R: Reports*, vol. 28, no. 1, pp. 1–63, 2000.

[5] T. Lan, P. D. Kaviratna, and T. J. Pinnavaia, "Epoxy self-polymerization in smectite clays," *Journal of Physics and Chemistry of Solids*, vol. 57, no. 6–8, pp. 1005–1010, 1996.

[6] M. A. Kumar, K. H. Reddy, Y. V. M. Reddy, G. R. Reddy, and S. V. Naidu, "Improvement of tensile and flexural properties in epoxy/clay nanocomposites reinforced with weave glass fiber reel," *International Journal of Polymeric Materials and Polymeric Biomaterials*, vol. 59, no. 11, pp. 854–862, 2010.

[7] M. V. Burmistr, K. M. Sukhyy, V. V. Shilov et al., "Synthesis, structure, thermal and mechanical properties of nanocomposites based on linear polymers and layered silicates modified by polymeric quaternary ammonium salts (ionenes)," *Polymer*, vol. 46, no. 26, pp. 12226–12232, 2005.

[8] J. H. Park and S. C. Jana, "Mechanism of exfoliation of nanoclay particles in epoxy-clay nanocomposites," *Macromolecules*, vol. 36, no. 8, pp. 2758–2768, 2003.

[9] A. A. Azeez, K. Y. Rhee, S. J. Park, and D. Hui, "Epoxy clay nanocomposites—processing, properties and applications: a review," *Composites Part B: Engineering*, vol. 45, no. 1, pp. 308–320, 2013.

[10] P. Kiliaris and C. D. Papaspyrides, "Polymer/layered silicate (clay) nanocomposites: an overview of flame retardancy," *Progress in Polymer Science*, vol. 35, no. 7, pp. 902–958, 2010.

[11] A. Leszczyńska, J. Njuguna, K. Pielichowski, and J. R. Banerjee, "Polymer/montmorillonite nanocomposites with improved thermal properties: part II. Thermal stability of montmorillonite nanocomposites based on different polymeric matrixes," *Thermochimica Acta*, vol. 454, no. 1, pp. 1–22, 2007.

[12] A. Tcherbi-Narteh, M. Hosur, E. Triggs, and S. Jeelani, "Thermal stability and degradation of diglycidyl ether of bisphenol A epoxy modified with different nanoclays exposed to UV radiation," *Polymer Degradation and Stability*, vol. 98, no. 3, pp. 759–770, 2013.

[13] R. P. Singh, M. Khait, S. C. Zunjarrao, C. S. Korach, and G. Pandey, "Environmental degradation and durability of epoxy-clay nanocomposites," *Journal of Nanomaterials*, vol. 2010, Article ID 352746, 13 pages, 2010.

[14] R. S. C. Woo, H. Zhu, C. K. Y. Leung, and J.-K. Kim, "Environmental degradation of epoxy-organoclay nanocomposites due to UV exposure: part II residual mechanical properties," *Composites Science and Technology*, vol. 68, no. 9, pp. 2149–2155, 2008.

[15] Q. Wang, C. Song, and W. Lin, "Study of the exfoliation process of epoxy-clay nanocomposites by different curing agents," *Journal of Applied Polymer Science*, vol. 90, no. 2, pp. 511–517, 2003.

[16] P. I. Xidas and K. S. Triantafyllidis, "Effect of the type of alkylammonium ion clay modifier on the structure and thermal/mechanical properties of glassy and rubbery epoxy-clay nanocomposites," *European Polymer Journal*, vol. 46, no. 3, pp. 404–417, 2010.

[17] J. M. Hutchinson, S. Montserrat, F. Román, P. Cortés, and L. Campos, "Intercalation of epoxy resin in organically modified montmorillonite," *Journal of Applied Polymer Science*, vol. 102, no. 4, pp. 3751–3763, 2006.

[18] A. Tcherbi-Narteh, M. V. Hosur, E. Triggs, and S. Jelaani, "Effects of surface treatments of montmorillonite nanoclay on cure behavior of diglycidyl ether of bisphenol a epoxy resin," *Journal of Nanoscience*, vol. 2013, Article ID 864141, 12 pages, 2013.

[19] F. Carrasco and P. Pagès, "Thermal degradation and stability of epoxy nanocomposites: influence of montmorillonite content and cure temperature," *Polymer Degradation and Stability*, vol. 93, no. 5, pp. 1000–1007, 2008.

[20] S. Montserrat, F. Román, J. M. Hutchinson, and L. Campos, "Analysis of the cure of epoxy based layered silicate nanocomposites: reaction kinetics and nanostructure development," *Journal of Applied Polymer Science*, vol. 108, no. 2, pp. 923–938, 2008.

[21] P. Pagès, T. Lacorte, M. Lipinska, and F. Carrasco, "Study of curing of layered silicate/trifunctional epoxy nanocomposites by means of FTIR spectroscopy," *Journal of Applied Polymer Science*, vol. 108, no. 4, pp. 2107–2115, 2008.

[22] A. Tcherbi-Narteh, M. Hosur, E. Triggs, P. Owuor, and S. Jelaani, "Viscoelastic and thermal properties of full and partially cured DGEBA epoxy resin composites modified with montmorillonite nanoclay exposed to UV radiation," *Polymer Degradation and Stability*, vol. 101, no. 1, pp. 81–91, 2014.

[23] V. Mittal, "Polypropylene-layered silicate nanocomposites: filler matrix interactions and mechanical properties," *Journal of Thermoplastic Composite Materials*, vol. 20, no. 6, pp. 575–599, 2007.

[24] ASTM, "Standard practice for plastics: dynamic mechanical properties: determination and report of procedures," ASTM 4065, ASTM International, West Conshohocken, Pa, USA, 2006.

[25] S. Vyazovkin, A. K. Burnham, J. M. Criado, L. A. Pérez-Maqueda, C. Popescu, and N. Sbirrazzuoli, "ICTAC Kinetics Committee recommendations for performing kinetic computations on thermal analysis data," *Thermochimica Acta*, vol. 520, no. 1-2, pp. 1–19, 2011.

[26] M. J. Starink, "The determination of activation energy from linear heating rate experiments: a comparison of the accuracy of isoconversion methods," *Thermochimica Acta*, vol. 404, no. 1, pp. 163–176, 2003.

[27] F. Román, S. Montserrat, and J. M. Hutchinson, "On the effect of montmorillonite in the curing reaction of epoxy nanocomposites," *Journal of Thermal Analysis and Calorimetry*, vol. 87, no. 1, pp. 113–118, 2007.

[28] Y.-N. Chan, T.-Y. Juang, Y.-L. Liao, S. A. Dai, and J.-J. Lin, "Preparation of clay/epoxy nanocomposites by layered-double-hydroxide initiated self-polymerization," *Polymer*, vol. 49, no. 22, pp. 4796–4801, 2008.

[29] T. B. Tolle and D. P. Anderson, "The role of preconditioning on morphology development in layered silicate thermoset nanocomposites," *Journal of Applied Polymer Science*, vol. 91, no. 1, pp. 89–100, 2004.

[30] D. W. Litchfield and D. G. Baird, "The rheology of high aspect ratio nanoparticles filled liquids," *Rheology Reviews*, pp. 1–60, 2006.

[31] K. Beazley, *Rheometry: Industrial Applications*, Edited by K. Walters, Research Studies Press, Chichester, UK, 1980.

[32] L. Le Pluart, J. Duchet, H. Sautereau, P. Halley, and J.-F. Gerard, "Rheological properties of organoclay suspensions in epoxy network precursors," *Applied Clay Science*, vol. 25, no. 3-4, pp. 207–219, 2004.

[33] S. T. Knauert, J. F. Douglas, and F. W. Starr, "The effect of nanoparticle shape on polymer-nanocomposite rheology and

tensile strength," *Journal of Polymer Science, Part B: Polymer Physics*, vol. 45, no. 14, pp. 1882–1897, 2007.

[34] R. Krishnamoorti, J. Ren, and A. S. Silva, "Shear response of layered silicate nanocomposites," *Journal of Chemical Physics*, vol. 114, no. 11, pp. 4968–4973, 2001.

[35] S. F. Zhao, G. P. Zhang, R. Sun, and C. P. Wong, "Curing kinetics, mechanism and chemorheological behavior of methanol etherified amino/novolac epoxy systems," *Express Polymer Letters*, vol. 8, no. 2, pp. 95–106, 2014.

[36] M. G. Lu, M. J. Shim, and S. W. Kim, "Curing reaction and phase change in a liquid crystalline monomer," *Macromolecular Chemistry and Physics*, vol. 202, no. 2, pp. 223–230, 2001.

[37] L. Barral, J. Cano, J. López et al., "Cure kinetics of amine-cured diglycidyl ether of bisphenol: a epoxy blended with poly(ether imide)," *Thermochimica Acta*, vol. 344, no. 1-2, pp. 127–136, 2000.

[38] P. J. Flory, *Principles of Polymer Chemistry*, Cornell University Press, Ithaca, NY, USA, 1953.

[39] H. Cai, P. Li, G. Sui et al., "Curing kinetics study of epoxy resin/flexible amine toughness systems by dynamic and isothermal DSC," *Thermochimica Acta*, vol. 473, no. 1-2, pp. 101–105, 2008.